The Crystal Structure of a Fusagenic Sperm Protein Reveals Extreme Surface Properties[†,‡]

Nicole Kresge,[§] Victor D. Vacquier,[||] and C. David Stout*[,§]

Department of Molecular Biology, The Scripps Research Institute, La Jolla, California 92037-1093, and Center for Marine Biotechnology and Biomedicine, Scripps Institution of Oceanography, University of California at San Diego, La Jolla, California 92093-0202

Received December 6, 2000; Revised Manuscript Received March 9, 2001

ABSTRACT: Sp18 is an 18 kDa protein that is released from abalone sperm during the acrosome reaction. It coats the acrosomal process where it is thought to mediate fusion between sperm and egg cell membranes. Sp18 is evolutionarily related to lysin, a 16 kDa abalone sperm protein that dissolves the vitelline envelope surrounding the egg. The two proteins were generated by gene duplication followed by rapid divergence by positive selection. Here, we present the crystal structure of green abalone sp18 resolved to 1.86 Å. Sp18 is composed of a bundle of five α-helices with surface clusters of basic and hydrophobic residues, giving it a large dipole moment and making it extremely amphipathic. The large clusters of hydrophobic surface residues and domains of high positive electrostatic surface charge explain sp18's ability as a potent fusagen of liposomes. The overall fold of sp18 is similar to that of green abalone lysin; however, the surface features of the proteins are quite different, accounting for their different roles in fertilization. This is the first crystal structure of a protein implicated in sperm−egg fusion during animal fertilization.

Protein-mediated membrane fusion is a ubiquitous event found in membrane trafficking, myotube formation, enveloped virus infection, secretory exocytosis, and fertilization. Most studies of membrane fusion have centered on viral fusion, which involves a conformational change in a viral protein resulting in the insertion of an amphipathic fusion peptide into the membrane to destabilize the lipid bilayer and initiate fusion (*1*). A less studied membrane fusion is that which occurs between gametes during fertilization. The two best-characterized proteins believed to be involved in sperm−egg fusion are sea urchin sperm bindin (*2*−*5*) and mouse egg CD9 (*6*−*9*). Bindin has a highly conserved 60-amino acid central domain that contains an 18-residue peptide that possesses all the fusagenic properties of the mature protein. In the presence of Zn^{2+}, this peptide, which contains three His residues, forms an amphipathic α-helix that fuses artificial lipid vesicles (*2*−*5*). Although it is unknown how CD9 mediates fusion in gametes, the eggs of mice whose CD9 is deleted are unable to fuse with sperm (*7*, *8*). CD9 has also been shown to facilitate fusion in other systems such as myoblast fusion (*10*) and viral infection (*11*, *12*). Rat sperm membrane protein DE is also reported to be fusagenic. However, DE has no hydrophobic domains and does not fuse liposomes, and the bulk of it is peripheral to the sperm cell membrane (*13*).

Abalone (a marine mollusk, genus *Haliotis*) sperm possess a large acrosomal granule containing roughly equal amounts of a 16 kDa protein named lysin and an 18 kDa protein, sp18 (*14*). Contact between the sperm and the egg vitelline envelope (VE)[1] triggers the acrosome reaction, which consists of the exocytotic release of both proteins and the elongation (by actin polymerization) of the acrosomal process. The dimeric lysin is deposited onto the surface of the egg VE where it binds to the VE receptor for lysin (VERL) and creates a hole in the VE by a species-specific, nonenzymatic mechanism (*15*). Sp18 coats the membrane covering the acrosomal process where it is thought to mediate sperm and egg cell membrane fusion (*16*). Lysin and sp18 were generated by gene duplication from an ancestral protein. Although lysin retains some ability to mediate membrane fusion, the more fusagenic sp18 is unable to dissolve the VE (*16*−*18*). Despite a common ancestry, lysin and sp18 have diverged substantially and have only 24 of 134 residues in common (Figure 1).

The sequences of sp18 from five species of abalone have been determined (*17*). The proteins vary in length from 132 to 146 residues, and all five have two conserved Cys residues. The sp18s are highly basic with calculated isoelectric points varying from 10.3 to 10.7. Only 11 residues are conserved among the five sp18s; however, polarity and size are conserved in amino acid replacements (*16*, *17*). Amino acid sequence divergence among sp18s is extraordinarily high; the level of sequence identity ranges from 27 to 87% with the average level of identity being 47%. While it is not known if sp18 contains a fusion peptide, it does contain five α-helices which are more amphipathic than honey bee venom melittin, one of the most potent membrane-disruptive peptides known (*16*, *19*). Sperm sp18 aggregates and fuses

[†] This research was supported by NSF Grant MCB-9816426 to C.D.S. and NIH Grant HD12986 to V.D.V.

[‡] The coordinates have been deposited in the Protein Data Bank as entry 1GAK.

* Corresponding author. Telephone: (858) 784-8738. Fax: (858) 784-2857. E-mail: dave@scripps.edu.

[§] The Scripps Research Institute.

[||] University of California San Diego.

[1] Abbreviations: VE, vitelline envelope; VERL, vitelline envelope receptor for lysin; CHES, 2-(*N*-cyclohexylamino)ethanesulfonic acid.

10.1021/bi002779v CCC: $20.00 © 2001 American Chemical Society
Published on Web 04/10/2001

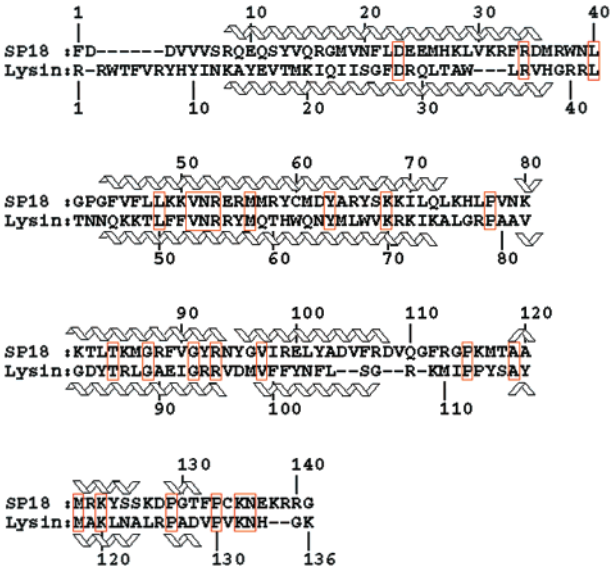

FIGURE 1: Sequence alignment of mature sp18 and lysin proteins from green abalone showing the locations of their α-helices as determined by X-ray crystallography. The 24 identical residues are boxed in red, and dashes have been inserted for optimal alignment.

negatively charged liposomes in a concentration-dependent manner (*16*).

To understand the basis of sp18's fusagenic ability and its structural relationship to lysin, we have determined the crystal structure of sp18 isolated from green abalone sperm. The structure reveals that sp18 is a monomer with an overall fold similar to that of lysin, and has surface features consistent with its putative role in membrane fusion.

EXPERIMENTAL PROCEDURES

Cross-Linking of Sp18. Sp18 was purified from green abalone sperm cells by CM cellulose chromatography (*16*, *17*), dialyzed into seawater with 0.04% sodium azide, and adjusted to a concentration of 0.04 mg/mL (2 μM). Aliquots of 12.5 μL of 1% DMSO in seawater were added to a series of microfuge tubes. A 2000 μM solution of the cross-linker disuccinimidyl suberate (DSS; Pierce Chemical Co.) was titered down in the microfuge tubes to 8 μM in 12.5 μL aliquots with a 50% dilution per transfer. Sp18 was added in 12.5 μL aliquots to each tube and allowed to react with DSS for 20 min. The reaction was stopped by the addition of 12.5 μL of 2× Laemmli sample buffer (*20*). The samples were electrophoresed on 12% polyacrylamide gels (SDS−PAGE) that were silver stained.

Protein Preparation and Crystallization. Purified sp18 was dialyzed against 50 mM sodium acetate (pH 4.9) and concentrated to 10 mg/mL. Two crystal forms of the protein were grown at 22 °C using the sitting drop vapor diffusion technique. A reservoir solution of 1 mL of 25% mPEG 5000, 200 mM ammonium acetate (pH 3.0), and 100 mM sodium phosphate and a drop ratio of 4 μL of protein solution to 11 μL of well solution produced hexagonal crystals. The crystals contained one molecule per asymmetric unit and belonged to space group $P6_5$. Smaller hexagonal crystals belonging to space group $P6_122$ were produced with a well solution of 1.0 M K^+/Na^+ tartrate, 100 mM CHES (pH 9.5), and 200 mM lithium sulfate and a drop ratio of 2:3. There was one molecule per asymmetric unit in this crystal form.

Heavy Atom Derivatives and Data Collection. For low-temperature data collection, crystals were frozen either in their mother liquor (pH 3 crystal form), or in mother liquor with 20% glycerol (pH 9.5 crystal form). Native data sets were collected for each crystal form at the Stanford Synchrotron Radiation Laboratory (SSRL; Table 1). The data were collected using a MAR image plate with monochromatic radiation with a wavelength of 0.98 or 1.08 Å. Data indexing and integration were carried out with MOSFLM (*21*), and scaling was carried out with SCALA (*21*). Heavy atom derivatives were prepared by soaking the pH 9.5 crystals in mother liquor containing either $KAuI_4$, K_2OsO_4, or $Pt(NH_3)_2Cl_2$ (Table 1). A xenon derivative was also prepared by incubating a pH 9.5 crystal in gaseous xenon under pressure (Table 1).

Structure Solution. Heavy atom sites in the pH 9.5 crystal form were determined using SOLVE (*22*−*25*) and XTALVIEW (*26*). Site refinement and phase calculations were carried out with SHARP (*27*), and density modification was carried out with DM (*21*). Phasing statistics are shown in Table 1.

The structure of the pH 3 crystal form was determined by molecular replacement using the pH 9.5 crystal form as a search model. The program AMoRe (*28*) gave one clear solution with a correlation coefficient of 25.9 after a cross-rotation function was performed in the resolution range of 12.0−3.5 Å. A translation function of this solution in the same resolution range gave a correlation coefficient of 47.3 and an *R* factor of 43.7%. Rigid body refinement yielded a final correlation coefficient of 61.1 and an *R* factor of 38.3%.

Model Building and Refinement. Because the platinum derivative of the pH 9.5 crystals diffracted to higher resolution than the native crystals, data from this derivative were used for refinement and model building. Map interpretation and model building were carried out with the program Xfit (*26*), and refinement was carried out with CNS (*29*). The progress of the refinement was monitored by 5% of the reflections used for the R_{free} calculation. Ten rounds of refinement were carried out with Xfit and CNS. Water molecules were added after the third round. Refinement statistics for the pH 9.5 crystal form are given in Table 2. Model building and refinement for the pH 3 crystal form were performed in a similar manner (Table 2). Water molecules were added after round 4. A total of 12 rounds of refinement were performed.

Coordinates and structure factors for the pH 3 structure have been deposited in the Protein Data Bank as entry 1GAK. GenBank accession numbers for green abalone (*Haliotis fulgens)* lysin and sp18 are M59972 and L36589, respectively.

Structural Analysis. Structural superpositions and calculations of rms deviations were carried out with the least-squares fit option in SHELXPRO (*30*). Solvent accessible areas were calculated with AREAIMOL and RESAREA (*21*). Calculations of surface areas and distances, and electrostatic surfaces, were carried out with GRASP (*31*). Calculations for percent surface area in basic residues (Table 4) were carried out using the residues Lys and Arg, while percent surface area in hydrophobic residues included Phe, Tyr, Ile, Met, Leu, and Trp. Percent surface area values were calculated for green abalone lysin (*32*), the melittin amphipathic α-helix (*33*), and myohemerythrin (*34*) as well as green abalone sp18.

Table 1: Data Collection and Phasing Statistics

	pH 3 form	pH 9.5 form	xenon	$KAuI_4$	K_2OsO_4	$Pt(NH_3)_2Cl_2$
space group	$P6_5$	$P6_122$	$P6_122$	$P6_122$	$P6_122$	$P6_122$
unit cell dimensions (Å)						
a	68.76	66.66	67.36	66.13	67.19	67.02
b	68.76	66.66	67.36	66.13	67.19	67.02
c	67.71	201.86	203.95	204.38	202.04	200.71
resolution (Å)	1.86	2.90	2.59	3.07	2.68	2.20
molecules per a.u.	1	1	1	1	1	1
multiplicity	5.4	4.8	4.2	5.0	3.5	3.3
$I/\sigma(I)$	8.0	9.6	10.6	8.3	8.8	12.5
final shell	2.4	1.9	2.5	2.4	3.2	2.4
completeness (%)	98.9	100	100	100	100	100
final shell	98.9	100	100	100	100	100
R_{sym} (%)[a]	6.8	7.4	5.8	6.8	5.4	4.5
final shell	31.1	40.3	30.4	31.6	24.2	31.0
derivatives[b]						
concentration	–	–	280 psi	10 mM	10 mM	10 mM
soaking time	–	–	1 h	5 days	5 days	7 days
no. of sites	–	–	1	1	1	3
R_{Cullis}[c]	–	–	87.3	87.2	83.8	70.1
phasing power[d]	–	–	1.36	1.49	1.39	1.53
figure of merit	–	–	0.41	0.50	0.44	0.46

[a] $R_{sym} = 100 \times \sum_h\sum_j|I_{hj} - I_h|/\sum_h\sum_j I_{hj}$, where I_h is the weighted mean intensity of the symmetry-related reflections I_{hj}. [b] Phasing statistics were calculated to 2.6 Å resolution. [c] $R_{Cullis} = 100 \times \sum_{hkl}|F_P \pm F_{PH}| - |F_{H,calc}|/\sum_{hkl}|F_P \pm F_{PH}|$. [d] Phasing power $= F_H/E$, where E is the estimated lack of closure.

Table 2: Refinement Statistics

	pH 3 form	pH 9.5 form
resolution (Å)	1.86	2.20
no. of reflections (unique/total)	15134/82274	25213/83327
no. of residues resolved	1−137	1−135
no. of non-hydrogen atoms	1294	1171
no. of water molecules	142	52
average *B* factor (Å^2)	26.5	36.3
R factor[a] (%)	22.7	25.4
R_{free}[b] (%)	24.7	28.7
Ramachandran statistics[c]		
most favored regions (%)	94.2	94.0
additional allowed regions (%)	5.8	6.0
generously allowed regions (%)	0.0	0.0
rms deviations from ideal geometry[d]		
bond distances (Å)	0.010	0.016
bond angles (deg)	1.38	1.68

[a] *R* factor $= \sum||F_{obs}| - |F_{calc}||/\sum|F_{obs}|$, where $|F_{obs}|$ and $|F_{calc}|$ are the observed and calculated structure factor amplitudes, respectively. [b] R_{free} is the *R* factor for a 5% subset of reflections not used in refinement. [c] As calculated with the program PROCHECK (*49*). [d] As calculated with the program WHATIF (*50*).

Table 3: Comparison of Green Abalone Sp18 and Lysin

	sp18	lysin[a]
dimensions (Å)	54 × 32 × 30	49 × 42 × 33
solvent accessible surface area (Å^2)	8171	7585
no. of hydrophobic residues [surface area (Å^2)]	39 (1802)	47 (1510)[b]
no. of basic residues [surface area (Å^2)]	32 (2960)	26 (2985)
dipole moment (eÅ)	88.47	38.71

[a] The calculations reflect an average of the A and B subunits of the green abalone lysin dimer (*32*). [b] Only residues 11−134 can be seen in the crystal structure of green abalone lysin, preventing hydrophobic residues Trp3, Phe5, Tyr8, and Tyr10 from being involved in this calculation.

RESULTS

Protein Fold. Sp18 is an elongated, three-sided molecule with approximate dimensions of 54 Å × 32 Å × 30 Å and a solvent accessible surface of 8171 Å^2. The molecule is 70% α-helical and contains no β-sheet. The helices form an up−down five-helix bundle with a right-handed twist (Figures 2A and 4). Helices α1−α4 form the core of the molecule and have extensive contacts with each other. A kink in the longest helix, helix α2, maximizes its contacts with helices 1, 3, and 4, while a bend between helices α3 and α4 promotes their tight interaction with the other helices. Helix α5, which is disrupted by two residues that form random coil (Lys127 and Asp128), extends away from the helical bundle. The last helix and the C-terminus are tethered to the core of the molecule by 11 hydrogen bonds and a left-handed disulfide bond. The disulfide bond exists between Cys60 and Cys134 and connects helix α5 at the C-terminus with helix α2.

Table 4: Molecular Amphipathicity Comparisons

molecule	% surface area in basic residues	% surface area in hydrophobic residues	total % amphipathic surface area
green abalone sp18	36	22	58
green abaone lysin	39	20	59
myohemerythrin	28	15	43
melittin α-helix	27	30	57

Comparison of Acidic and Basic Crystal Forms of Sp18. The pH 9.5 and pH 3 crystal forms of sp18 have nearly identical overall folds. A superposition of the two molecules results in an rms deviation of 0.67 Å for the α-carbon backbone, and 1.50 Å for all atoms. The structures differ mostly at the N- and C-termini and in the turns between helices α1 and α2 and between helices α4 and α5. These differences most probably arise from differences in crystal packing rather than from the change in pH. In the pH 9.5 crystal form of sp18, the majority of the contacts with symmetry-related molecules occur in residues in the turns between helices α1 and α2 and between helices α4 and α5, while the termini and the other helices make very few contacts. The pH 3 crystal form of sp18, on the other hand,

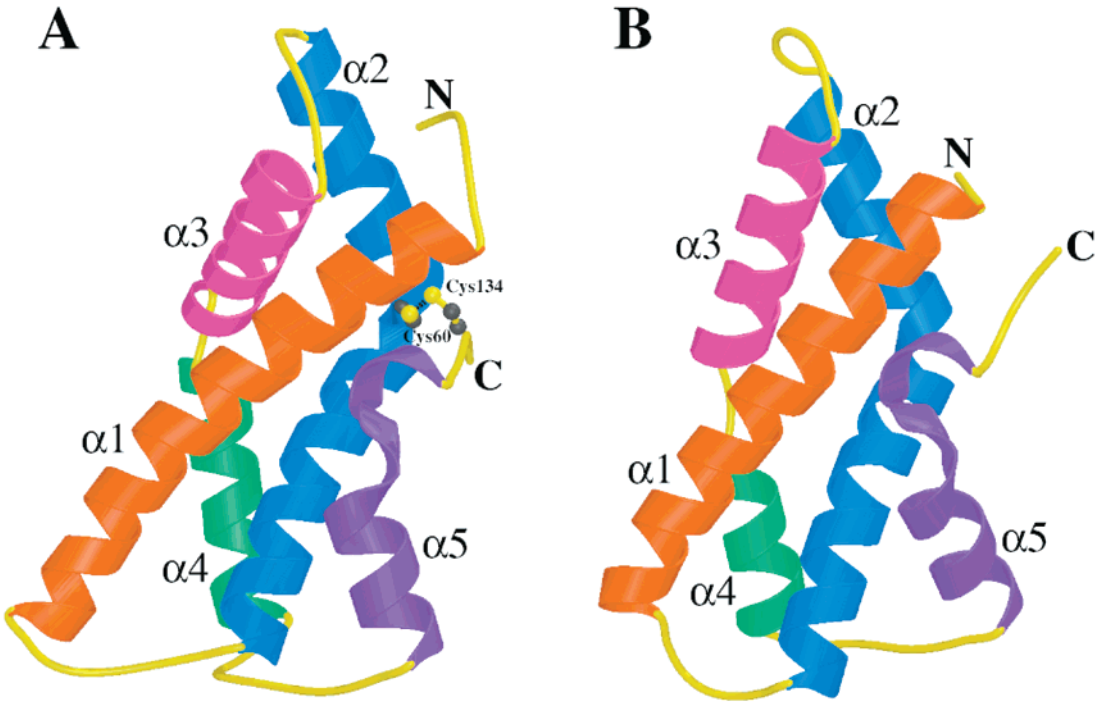

FIGURE 2: Comparison of the folds of sp18 (A) and lysin (B) from green abalone (*32*). The α-carbon ribbon diagram of sp18 shows the disulfide bond between Cys60 and Cys134 in yellow.

forms extensive contacts throughout the molecule with neighboring molecules. Many of these contacts also exist in the turns between helices α1 and α2 and between helices α4 and α5. Thus, the different contacts at the turns and termini probably result in the minor differences seen between the two molecules. Since both crystal forms are virtually identical, all further analysis was carried out on the higher-resolution pH 3 model.

Surface Features. Green abalone sp18 has 39 hydrophobic and aromatic amino acids, 29 of which are found on the surface of the molecule where they contribute 22% of the total surface area (Tables 3 and 4 and Figure 3A−C), a remarkably large hydrophobic area for a small, soluble, globular protein. When mapped onto the surface of sp18, all but three of these surface residues are confined to two of sp18's three faces (Figure 3B,C).

Sp18's 32 Arg and Lys residues occupy 36% of its total surface area (Tables 3 and 4). The basic residues are found mostly on one face of the protein (Figure 3D). The face opposite the one containing the basic residues exhibits a distinct acidic ridge consisting of eight residues, Asp2, Asp3, Glu54, Asp62, Glu100, Asp104, Asp108, and Glu137 (Figure 3F). As a result, sp18 has a very large molecular dipole moment of 88.47 eÅ (Table 3). The dipole passes normal to the helical bundle in the direction of the most basic surface, and opposite the surface containing the most exposed hydrophobic residues (Figure 3B,C) and the acidic patch (Figure 3D,E).

Molecular Amphipathicity. The surface of sp18 with the greatest amount of positive charge (Figure 3D) has very few hydrophobic residues (Figure 3A), while the surfaces with the most hydrophobic residues (Figure 3B,C) have the least amount of positive charge (Figure 3E,F). This distribution of residues results in an extremely amphipathic protein. Although all of sp18's α-helices are very amphipathic themselves (*16*), this unusual distribution of amino acids is

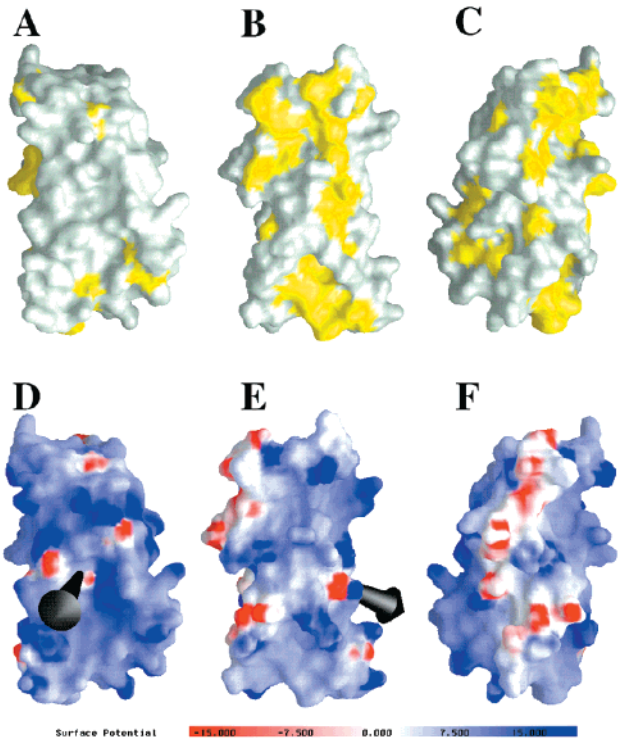

FIGURE 3: Surface features of sp18 showing its three sides (surface B is a 135° rotation from A, and surface C is a 60° rotation from B). Surfaces A−C depict the locations of the hydrophobic residues (yellow). Surfaces D−F show the electrostatic potential of the same surface as A−C and the direction of the net dipole moment (arrow). The deepest shades of blue and red correspond to potentials of 15 and −15 kT/e, respectively. Electrically neutral surfaces are white. The orientations of surfaces A and D are approximately the same as in Figure 2.

due to the overall polypeptide fold. In comparisons of the percentage of protein surface area occupied by basic and hydrophobic residues, sp18 has more basic and hydrophobic

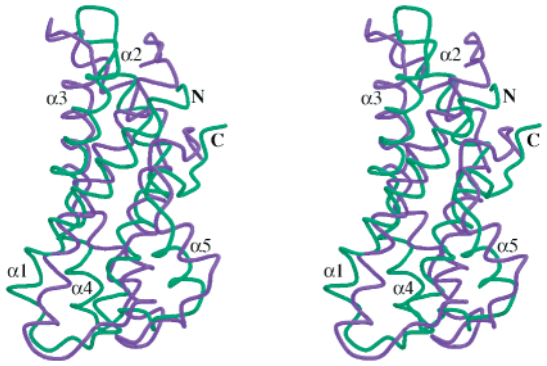

FIGURE 4: Stereoview of sp18 (purple) and lysin (green) α-carbon superposition. Areas with the least similarity include the N- and C-terminal residues as well as helix α5 and the turn between helices α4 and α5.

surface area than myohemerythrin (Table 4), indicating that sp18 does not have surface properties similar to those of this soluble, helical bundle protein. The melittin α-helix, one of the most amphipathic helical peptides known (*33*), has less basic surface area and more hydrophobic surface area than sp18 (Table 4). However, the total surface area occupied by these amphipathic residues is about equal to that of sp18, suggesting that, overall, sp18 is as amphipathic as melittin. This feature would be consistent with the fusagenic properties of sp18.

Comparison to Lysin. Alignment of mature sp18 and lysin amino acid sequences from *H. fulgens* (Figure 1) shows the two proteins are identical in only 24 of 136−141 positions (17−18%). Although sp18 is slightly larger than lysin (Table 3), the crystal structures display almost identical placement of the five α-helices in both proteins (*32*; Figures 1, 2, and 4). Comparison of α-carbon backbones shows that the overall folds of lysin and sp18 are nearly identical, substantiating their generation by gene duplication (Figures 2 and 4).

Despite a striking similarity in overall fold (Figures 2 and 4), the structures of sp18 and lysin differ significantly in the relative angles of their helices. The rms deviation for the superposition of sp18 α-carbon atoms onto those of lysin is 6.45 Å, and the rms deviation for a superposition of all atoms is 6.78 Å. In general, the helices of sp18 are more loosely packed than those of lysin. The greatest variability between the two structures is found in helix α5 and in the turn between helices α4 and α5, most probably because the disulfide bond that joins helices α2 and α5 in sp18 is not found in lysin (Figures 2 and 4). As a result, the C-terminus is much closer to helix α2 in sp18 than in lysin (4.9 vs 6.8 Å), and the overall mobility of the C-terminus, as measured by temperature factor, is much lower in sp18 than in lysin (28.9 vs 54.2 Å^2). Another difference between the two proteins is that sp18 is a prismatic, three-sided molecule (Figure 3) while lysin is a flat molecule with two broad faces and two narrow faces (*32*, *35*).

Like sp18, green abalone lysin is an amphipathic molecule. Fifteen of lysin's hydrophobic and aromatic residues are confined to one of its flat faces, forming a hydrophobic patch (*32*). Lysin's other face contains the majority of its 26 Arg and Lys residues which form two parallel tracks of basic residues (*32*). These residues contribute approximately 39% of the total surface area (Tables 3 and 4). Sp18 has more basic residues, a similarly sized basic surface, but a dipole moment greater than twice that of lysin's (Table 3). Although sp18 has a smaller number of hydrophobic and aromatic residues, more of them are exposed to solvent, resulting in a larger hydrophobic surface (Tables 3 and 4). Thus, although the overall polypeptide folds of sp18 and lysin are very similar (Figures 2 and 4), sp18's surface features and net dipole are more extreme than those of lysin.

Sp18 Is a Monomer. Both the pH 3 and pH 9.5 crystal forms of sp18 reveal a monomeric protein. Lysin, on the other hand, crystallizes as a monomer at basic pH and as a dimer at acidic pH (*32*, *35*). Dimerization occurs via the intercalation of conserved hydrophobic patch residues from each lysin monomer (*32*, *35*). Sequence alignment shows that the residues involved in lysin dimerization are not present in sp18 (*32*, *35*, *36*). Superposition of sp18 onto the lysin dimer crystal structure reveals the residues that would be involved in forming the sp18 dimer are not of the correct charge and do not possess the characteristics to form the necessary interactions needed for dimerization. Cross-linking experiments which showed that lysin is a dimer at concentrations of >2 μM (*35*) indicated that sp18 exists only as only a monomer.

DISCUSSION

Although green abalone sp18 and lysin have only 24 residues in common, their tertiary folds are remarkably similar, confirming their ancestral relationship (Figures 1, 2, and 4). However, their amino acid sequences are currently so extensively diverged that neither protein will match with the other using a standard BLAST or PSI-BLAST search of GenBank (*17*). However, a PROFILESEARCH using sp18 sequences of five abalone species as input does yield significant GenBank matches with abalone sperm lysins (*17*). In addition to the dissimilarity in amino acid sequences, the disulfide bond in sp18 is conserved in all five species, whereas Cys residues are completely absent in the sequences of mature lysins from 20 abalone species (*37*).

The divergence of sp18's and lysin's primary sequences has resulted in two molecules with similar overall folds that have surfaces specialized for different functions. Lysin dissolves the VE by binding to VERL as a dimer and interacting with its receptor via its hydrophobic and basic residues (*32*). Thus, an essential part of this recognition and dissolution process is the interaction of the lysin dimer with its receptor (*38*, *39*). The fact that sp18 does not form a dimer is consistent with its distinct function compared to lysin. Furthermore, the C-terminus of lysin is involved in the initial recognition between lysin and VERL (*40*). In sp18, the C-terminus is less mobile due to the constraints imposed by the disulfide bond, and may not interact with other molecules as easily as lysin's C-terminus.

Sp18 is a potent fusagen of negatively charged liposomes and is most probably involved in fusing egg and sperm cell membranes (*16*). Its amphipathic surface and crystal structure suggest how sp18 has evolved into such an excellent fusagen. The high concentration of basic residues and resulting large dipole moment would be beneficial in interactions with negatively charged phospholipid headgroups in the membrane, while sp18's large hydrophobic surface is ideal for binding to the fatty acid molecules of the lipid bilayer.

Molecules with amphipathic features similar to those of sp18 are commonly involved in membrane interactions.

Melittin, which consists of two α-helical segments, is a small water-soluble peptide that spontaneously integrates into lipid bilayers. One side of the molecule contains 10 apolar residues, while the opposite face contains four polar side chains (*33*). The pore-forming domain of Colicin A consists of 10 α-helices organized into a three-layer structure. A ring of eight basic residues orients the molecule perpendicular to the membrane surface, while hydrophobic residues penetrate the membrane (*41*). The T-domain of diphtheria toxin consists of nine α-helices arranged in three layers. The outermost layer contains a high density of charged residues that serve as the initial site of contact with the negatively charged membrane. Exposure to the acidic lumen of the endosome triggers a pH-induced partial unfolding of the domain, resulting in its insertion into the membrane (*42*, *43*). However, sp18 differs from this molecule in that its crystal structures at acidic and basic pH indicate it only undergoes minor pH-induced conformational changes. And finally, the vinculin tail consists of five amphipathic helices that form an antiparallel bundle. The surface of the vinculin molecule contains a ladder of basic residues and a basic collar surrounding a hydrophobic C-terminal hairpin; both features are proposed to interact with the membrane in a manner similar to that of sp18 (*44*).

The presence of a disulfide bond in sp18 may be important for its fusagenic activity. Previous studies on sp18 showed that its helices are extremely amphipathic (*16*). But, unlike many proteins, several of the hydrophobic residues are exposed to solvent. The disulfide bond between helix α2 and the C-terminus may prevent sp18 from unfolding, forcing hydrophobic residues to remain exposed to solvent. On the other hand, the potential to unfold could be used by sp18 to fuse sperm and egg cell membranes. Most fusion proteins undergo a conformational change resulting in the insertion of an amphipathic α-helix into the membrane. Freeze-fracture-deep-etch replicas of the abalone egg surface show that it is covered by a coat of fibers to which the sperm bind (*45*). Hypothetically, these fibers could contain a protein disulfide isomerase that could function as a receptor for sp18. Protein disulfide isomerases have been found on cell surfaces, where they are involved in the cleavage of disulfide bonds (*46*−*48*). Perhaps the interaction between sp18 and a disulfide isomerase severs the disulfide bond, causing sp18 to spring open and insert amphipathic helices into the egg membrane.

ACKNOWLEDGMENT

We thank P. Kuhn, S. M. Soltis, and A. Cohen for help at SSRL beamlines 7-1 and 9-1, P. A. Williams for assistance with data collection, and W. J. Swanson for discussions. This work is based on research conducted at the Stanford Synchrotron Radiation Laboratory (SSRL), which is funded by the Department of Energy, Office of Basic Energy Sciences. The Biotechnology Program is supported by the National Institutes of Health, National Center for Research Resources, Biomedical Technology Program, and the Department of Energy, Office of Biological and Environmental Research.

REFERENCES

1. Hernandez, L. D., Hoffman, L. R., Wolfsberg, T. G., and White, J. M. (1996) *Annu. Rev. Cell Dev. Biol. 12*, 627−661.
2. Ulrich, A. S., Otter, M., Glabe, C. G., and Hoekstra, D. (1998) *J. Biol. Chem. 273*, 16748−16755.
3. Ulrich, A. S., Tichelarr, W., Forster, G., Zschornig, O., Weinkauf, S., and Meyer, H. W. (1999) *Biophys. J. 77*, 829−841.
4. Glaser, R. W., Grune, M., Wandelt, C., and Ulrich, A. S. (1999) *Biochemistry 38*, 2560−2569.
5. Binder, H., Arnold, K., Ulrich, A. S., and Zschornig, O. (2000) *Biochim. Biophys. Acta 1468*, 345−358.
6. Chen, M. S., Tung, K. S. K., Coonrod, S. A., Takahashi, Y., Biger, D., Chang, A., Yamashita, Y., Kincade, P. W., Herr, J. C., and White, J. M. (1999) *Proc. Natl. Acad. Sci. U.S.A. 96*, 11830−11835.
7. Kaji, K., Oda, S., Shikano, T., Ohnuki, T., Uematsu, Y., Sakagami, J., Tada, N., Miyazaki, S., and Kudo, A. (2000) *Nat. Genet. 24*, 279−282.
8. Le Naour, F., Rubinstein, E., Jasmin, C., Prenant, M., and Boucheix, C. (2000) *Science 287*, 319−321.
9. Miyado, K., Yamada, G., Yamada, S., Hasuwa, H., Nakamura, Y., Ryu, F., Suzuki, K., Koai, K., Inoue, K., Ogura, A., Okabe, M., and Mekada, E. (2000) *Science 287*, 321−324.
10. Tachibana, I., and Hemler, M. E. (1999) *J. Cell Biol. 146*, 893−904.
11. Loffler, S., Lottspeich, F., Lanza, F., Azorsa, D. O., ter Meulen, V., and Schneider-Schaulies, J. (1997) *J. Virol. 71*, 42−49.
12. Willett, B., Hosie, M., Shaw, A., and Neil, J. (1997) *J. Gen. Virol. 78*, 611−618.
13. Cohen, D. J., Rochwerger, L., Ellerman, D. A., Morgenfeld, M. M., Busso, D., and Cuasnicu, P. S. (2000) *Mol. Reprod. Dev. 56*, 180−188.
14. Lewis, C. A., Talbot, C. F., and Vacquier, V. D. (1982) *Dev. Biol. 92*, 227−239.
15. Vacquier, V. D., Swanson, W. J., Metz, E. C., and Stout, C. D. (1999) *Adv. Dev. Biochem. 5*, 49−81.
16. Swanson, W. J., and Vacquier, V. D. (1995) *Biochemistry 34*, 14202−14208.
17. Swanson, W. J., and Vacquier, V. D. (1995) *Proc. Natl. Acad. Sci. U.S.A. 92*, 4957−4961.
18. Hong, K., and Vacquier, V. D. (1986) *Biochemistry 25*, 543−549.
19. Fujii, G., Selsted, M. E., and Eisenberg, D. (1993) *Protein Sci. 2*, 1301−1312.
20. Laemmli, U. K. (1970) *Nature 277*, 680−685.
21. Collaborative Computational Project Number 4 (1994) *Acta Crystallogr. D50*, 760−763.
22. Terwilliger, T. C., and Eisenberg, D. (1983) *Acta Crystallogr. A39*, 813−817.
23. Terwilliger, T. C., Kim, S.-H., and Eisenberg, D. (1987) *Acta Crystallogr. A43*, 1−5.
24. Terwilliger, T. C., and Eisenberg, D. (1987) *Acta Crystallogr. A43*, 6−13.
25. Terwilliger, T. C., and Berendzen, J. (1996) *Acta Crystallogr. D52*, 749−757.
26. McRee, D. E. (1999) *J. Struct. Biol. 125*, 156−165.
27. De La Fortelle, E., and Bricogne, G. (1997) *Methods Enzymol. 276*, 472−493.
28. Navaza, J., and Saludjian, P. (1997) *Methods Enzymol. 276*, 581−594.
29. Brünger, A. T., Adams, P. D., Clore, G. M., DeLano, W. L., Gros, P., Grosse-Kunstleve, R. W., Jiang, J.-S., Kuszewski, J., Nilges, M., Pannu, N. S., Read, R. J., Rice, L. M., Simonson, T., and Warren, G. L. (1998) *Acta Crystallogr. D54*, 905−921.
30. Sheldrick, G. M., and Schneider, T. R. (1997) *Methods Enzymol. 276*, 319−343.
31. Nicholls, A., Sharp, K. A., and Honig, B. (1991) *Proteins: Struct., Funct., Genet. 11*, 281−296.
32. Kresge, N., Vacquier, V. D., and Stout, C. D. (2000) *J. Mol. Biol. 296*, 1225−1234.
33. Terwilliger, T. C., and Eisenberg, D. (1982) *J. Biol. Chem. 257*, 6016−6022.

34. Sheriff, S., Hendrickson, W. A., and Smith, J. L. (1987) *J. Mol. Biol. 197*, 273.
35. Shaw, A., Fortes, P. A. G., Stout, C. D., and Vacquier, V. D. (1995) *J. Cell Biol. 130*, 1117−1125.
36. Kresge, N., Vacquier, V. D., and Stout, C. D. (2000) *Acta Crystallogr. D56*, 34−41.
37. Lee, Y.-H., Ota, T., and Vacquier, V. D. (1995) *Mol. Biol. Evol. 12*, 231−238.
38. Swanson, W. J., and Vacquier, V. D. (1997) *Proc. Natl. Acad. Sci. U.S.A. 94*, 6724−6729.
39. Swanson, W. J., and Vacquier, V. D. (1998) *Science 281*, 710−712.
40. Lyon, J. D., and Vacquier, V. D. (1999) *Dev. Biol. 214*, 151−159.
41. Parker, M. W., Postma, J. P. M., Pattus, F., Tucker, A. D., and Tsernoglou, D. (1992) *J. Mol. Biol. 224*, 639.
42. Choe, S., Bennett, M. J., Fujii, G., Curmi, P. M. G., Kantardjieff, K. A., Collier, R. J., and Eisenberg, D. (1992) *Nature 357*, 216−222.
43. Zhan, H., Choe, S., Huynh, P. D., Finkelstein, A., Eisenberg, D., and Collier, R. J. (1994) *Biochemistry 33*, 11254−11263.
44. Bakolitsa, C., Pereda, J. M., Bagshaw, C. R., Critchley, D. R., and Liddington, R. C. (1999) *Cell 99*, 601−613.
45. Mozingo, N. M., Vacquier, V. D., and Chandler, D. E. (1995) *Mol. Reprod. Dev. 41*, 493−502.
46. Pariser, H. P., Zhang, J., and Hausman, R. E. (2000) *Exp. Cell Res. 258*, 42−52.
47. Mandel, R., Ryser, H. J., Ghani, F., Wu, M., and Peak, D. (1993) *Proc. Natl. Acad. Sci. U.S.A. 90*, 4112−4116.
48. Terada, K., and Manchikalapudi, P. (1995) *J. Biol. Chem. 270*, 20410−20416.
49. Laskowski, R. A., MacArthur, M. W., Moss, D. S., and Thornton, J. M. (1993) *J. Appl. Crystallogr. 24*, 946−950.
50. Hooft, R. W. W., Vriend, G., Sander, C., and Abola, E. E. (1996) *Nature 381*, 272.

BI002779V